Molecular Crystals and Liquid Crystals
Publication details, including instructions for authors and subscription information:
http://www.tandfonline.com/loi/gmcl20

Supramolecular Liquid Crystals Induced by Intermolecular Hydrogen Bonding

Huidan Lu [a], Jianxiu Wang [a] & Xiangzhi Song [b]

[a] School of Chemistry and Chemical Engineering, Central South University, Changsha, Hunan, P. R. China

[b] Rowland Institute at Harvard, Harvard University, Cambridge, Massachusetts, USA

Version of record first published: 08 Apr 2011

To cite this article: Huidan Lu, Jianxiu Wang & Xiangzhi Song (2011): Supramolecular Liquid Crystals Induced by Intermolecular Hydrogen Bonding, Molecular Crystals and Liquid Crystals, 537:1, 93-102

To link to this article: http://dx.doi.org/10.1080/15421406.2011.556512

Mol. Cryst. Liq. Cryst., Vol. 537: pp. 93–102, 2011

ISSN: 1542-1406 print/1563-5287 online
DOI: 10.1080/15421406.2011.556512

Taylor & Francis
Taylor & Francis Group

Supramolecular Liquid Crystals Induced by Intermolecular Hydrogen Bonding

HUIDAN LU,[1] JIANXIU WANG,[1] AND XIANGZHI SONG[2]

[1]School of Chemistry and Chemical Engineering, Central South University, Changsha, Hunan, P. R. China
[2]Rowland Institute at Harvard, Harvard University, Cambridge, Massachusetts, USA

A series of new hydrogen-bonded liquid-crystal complexes formed between para-substitued alkoxybenzoic acids (OBAm, where m denotes the number of the carbon in the alkoxy group, m = 4, 5, 6, 7, 8, 10) and 4′-pyridylazophenyl-4-alkoxybenzoate (PEAPn, where n represents the number of the carbon in the alkoxy group, n = 5, 6, 7 8, 10, 12, 14, 16) have been investigated by Fourier transform infrared (FTIR) Spectroscopy, differential scanning calorimetry (DSC), Polarizing optical microscopy (POM), and variable-temperature X-ray diffraction analysis. All PEAPn themselves are smectic mesogens and the hydrogen-bonded complexes show entiotropic smectic phases. The hydrogen bonding can raise the clear points of the complexes and, at the same time, decrease the melting points. The complexes were found to possess a much wider mesophase range than their corresponding individual components. The influence of the terminal chain lengths of OBAm and PEAPn on the phase transition temperatures is discussed. The results indicate that mostly the mesogenic behavior of the hydrogen-bonded assemblies exhibits a slight odd–even effect.

Keywords Azo dyes; hydrogen-bonded; liquid crystals; smectic

Introduction

Hydrogen bonding, one of the most important interactions in nature, plays a significant role in molecular recognition and self-assembly [1]. Originally, Jones and coworkers discovered that 4-substituted benzoic acids themselves showed liquid-crystal phases [2,3]. Later, Kato and Frechet enlarged the hydrogen-bonded liquid-crystal systems by assembling 4-alkoxybenzoic acids with pyridine derivatives, which led to increased interests in the study of hydrogen-bonded liquid crystals [4]. Since then, a large number of supramolecular hydrogen-bonded mesogenic materials have been synthesized and their properties have been thoroughly investigated [5–13]. To date, hydrogen-bonded liquid crystals are an actively investigated research area.

Address correspondence to Xiangzhi Song, Rowland Institute at Harvard, Harvard University, Cambridge, MA 02142. E-mail: song@rowland.harvard.edu or Jianxiu Wang, School of Chemistry and Chemical Engineering, Central South University, Changsha, Hunan, P.R. China, 410083. E-mail: jxiuwang@mail.csu.edu.cn

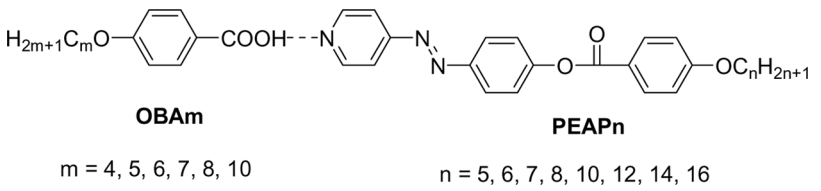

Scheme 1. Molecular structures of the compounds studied and their acronyms.

Azo dyes, as an important type of dye in guest–host liquid-crystal display (LCD) applications, can improve the viewing angle as well as the order parameter and provide full-color reflective displays. In recent years, azo dyes have drawn considerable attention due to their potential application in optical storage systems [14–17]. However, there are still some problems with the azo dyes in the guest–host LCD system such as solubility, stability, and viscosity [18,19]. To some extent, azo dyes themselves as liquid crystals can potentially resolve the above problems. Previously, we reported self-assembled azo dye liquid crystals through hydrogen bonding [20]. More work in this area was carried out by Mallia *et al.* [21]. Recently, Naoum *et al.* have reported new examples of H-bonded liquid-crystal complexes [22,23]. In order to expand Naoum *et al.'s* study and perform a systematic study, herein we synthesized a series of PEAPn (n = 5, 6, 7, 8, 10, 12, 14, 16) and thoroughly investigated their corresponding hydrogen-bonded liquid crystal complexes formed with *para*-substitued alkoxybenzoic acids (OBAm, m = 4, 5, 6, 7, 8, 10). We expect to find out the relationship between the liquid-crystalline properties of the complexes and the terminal chain length of the alkoxy group in the hydrogen donors, OBAm, and the acceptors, PEAPn, respectively. The structures of these hydrogen-bonded liquid crystals are shown in Scheme 1.

Experimental

The synthetic route for the PEAPn investigated is depicted in Scheme 2.

Synthesis of 4-Alkoxybenzoic Acids

The benzoic acids with shorter chains including OBA4, OBA5, OBA6, OBA7, and OBA8 were synthesized as follows: 0.1 mol of 4-hydroxybenzoic acid and 0.1 mol of the corresponding bromoalkanes were dissolved in 100 mL of anhydrous ethanol. To the above solution, 0.2 mol of KOH was added as base. The mixture was heated to reflux for 4 h under stirring. After cooling to room temperature, the mixture was acidified with 1 N hydrochloric acid to yield white precipitates. After filtration, recrystallization in ethanol/water (V:V = 1:1) gave the pure product. OBA10 was

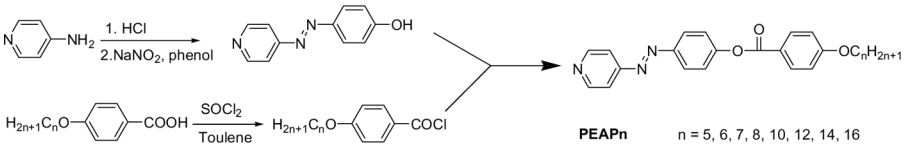

Scheme 2. Synthetic route of the PEAPn.

synthesized by the following procedure: in a 250-mL round-bottom flask, 0.1 mol of ethyl 4-hydroxybenzoate and 0.1 mol of bromodecane were dissolved in 100 mL of dimethylformamide (DMF), followed by addition of 0.1 mol of anhydrous K_2CO_3 as base and a small amount of potassium iodide (KI) as catalyst. The mixture was then heated to 100°C for 6 h under stirring. After cooling to room temperature, 100 mL of ice water was added to give precipitates. The precipitates were collected after filtration and then hydrolyzed in 100 mL of ethanol containing 0.12 mol of KOH. Acidification using 1 N hydrochloric acid gave a crude product as a white solid. A pure product could be obtained through recrystallization in ethanol/water (V:V = 1:1) co solvent.

All alkoxybenzoic acids were characterized by elemental analysis and mass spectrometry.

Synthesis of 4-Hydroxyazopyridine

4-Hydroxyazopyridine was prepared from 4-aminopyridine and phenol. To a solution of $NaNO_2$ (4.0 g) in water (20 mL), phenol (5 g) in 10% NaOH solution (45 mL) was added. At 0°C, the mixture was added to a solution of 4-aminopyridine (6 g) in hydrochloric acid (25 mL of concentrated HCl:16 mL of water) under stirring in 10 min. The solution was then adjusted to pH about 6 using saturated aqueous Na_2CO_3 solution to give yellow precipitates. After filtration and drying in air, the crude product was used directly for the next reaction without further purification (about 75% of yield).

Synthesis of PEAPn

The alkoxybenzoic acid (0.005 mol) was dissolved in a solution of thionyl chloride (5 mL) in toluene (10 mL). The mixture was heated to reflux for 3 h under stirring. After cooling to room temperature, the excess thionyl chloride and toluene were removed via evaporation to yield the alkoxybenzoic chloride.

The prepared alkoxybenzoic chloride and 4-hydroxyphenylazopyridine (1.0 g) were dissolved in pyridine (20 mL). The mixture was heated to reflux for 3 h. After

Table 1. Results of yield, mass spectra, and elemental analysis of PEAPn

			Elemental analysis					
			Calculated			Experimental		
PEAPn	M/z	Yield (%)	C	H	N	C	H	N
PEAP5	389	60	70.92	5.96	10.79	70.78	5.899	10.74
PEAP6	403	65	71.43	6.25	10.42	70.83	6.123	10.34
PEAP7	417	67	71.91	6.52	10.07	71.53	6.187	10.34
PEAP8	431	70	72.35	6.78	9.74	72.02	6.625	9.692
PEAP10	459	59	73.16	7.24	9.15	72.91	7.193	9.123
PEAP12	487	55	73.88	7.65	8.62	73.89	7.514	8.513
PEAP14	515	54	74.52	8.02	8.15	74.28	7.863	8.033
PEAP16	543	56	75.09	8.35	7.73	74.98	8.210	7.707

Table 2. Data of ^{1}H NMR spectra of PEAPn (400 MHz in $CDCl_3$)

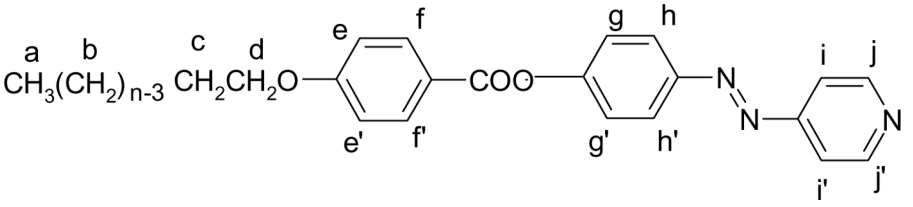

n	a	b	c	d	ee′	ff′	gg′	hh′	ii′	jj′
5	0.9368	1.4003–1.4799	1.8429	4.0596	8.1569	7.7201	8.0629	6.9881	7.4083	8.8307
6	0.9313	1.3477–1.4902	1.8311	4.0558	8.1551	7.7151	8.0599	6.9860	7.4063	8.8280
7	0.9250	1.3540–1.4862	1.8382	4.0633	8.1862	7.7830	8.0564	6.9733	7.4016	8.8396
8	0.8982	1.3035–1.5033	1.8328	4.0569	8.1687	7.7342	8.0632	6.9997	7.4080	8.8296
10	0.8895	1.2831–1.5013	1.8321	4.0569	8.1734	7.7461	8.0660	6.9870	7.4228	8.8386
12	0.8857	1.2720–1.5004	1.8309	4.0552	8.1678	7.7439	8.0637	6.9862	7.4209	8.8377
14	0.8833	1.2670–1.5005	1.8313	4.0554	8.1556	7.7295	8.0506	6.9862	7.4080	8.8304
16	0.8810	1.2629–1.5002	1.8307	4.0547	8.1553	7.7323	8.0629	6.9981	7.4203	8.8303

cooling to room temperature, the mixture was poured into 100 mL of cold ice water. The orange precipitates were collected after filtration and then purified by silica gel column chromatography (chloroform:acetone = 5:1 as the eluent). The overall yields of all the PEAPn were 56–70%.

All PEAPn were characterized by ^{1}H-nuclear magnetic resonance (NMR), elemental analysis, and mass spectrometry. The data are summarized in Tables 1 and 2.

Preparation of the Hydrogen-Bonded Complexes

Forty-eight hydrogen-bonded complexes were obtained via the slow evaporation of the tetrahydrofuran (THF) solution containing hydrogen acceptors (PEAPn) and hydrogen donors (OBAm) in a molar ratio of 1:1. The compounds were subsequently dried under vacuum to remove the solvent completely.

Results and Discussion

Thermal Properties of PEAPn

The thermal behaviors of all PEAPn were identified by differential scanning calorimetry (DSC) and polarizing optical microscopy (POM). All PEAPn themselves show liquid-crystal phases. Among them, PEAP6 and PEAP7 are monotropic smectic liquid crystals, and the remaing PEAPn are entiotropic smectic mesogens. The smectic phases were determined by their typical homeotropic textures. PEAP8 exhibited two smectic phases, one appearing with a typical homeotropic texture at high temperature and the other appearing with a typical focal-conic texture at low temperature. The thermal behaviors of PEAPn are summarized in Table 3. It should be noted that alkoxyphenylazopyridines, analogues of PEAPn, were not mesogenic according to our previous study [20]. The introduction of one more benzene ring to

Table 3. Phase transition temperatures of PEAPn

PEAP5	Cr	$\underset{95.49^{o}C}{\overset{94.97^{o}C}{\rightleftharpoons}}$	Cr'	$\underset{}{\overset{115.40^{o}C}{\rightleftharpoons}}$	Sm	$\underset{140.62^{o}C}{\overset{142.02^{o}C}{\rightleftharpoons}}$	I	
PEAP6	Cr	$\underset{118.93^{o}C}{\overset{142.49^{o}C}{\rightleftharpoons}}$	Sm	$\underset{140.91^{o}C}{\overset{}{\rightleftharpoons}}$	I			
PEAP7	Cr	$\underset{114.60^{o}C}{\overset{144.37^{o}C}{\rightleftharpoons}}$	Sm	$\underset{136.75^{o}C}{\overset{}{\rightleftharpoons}}$	I			
PEAP8	Cr	$\underset{96.14^{o}C}{\overset{108.04^{o}C}{\rightleftharpoons}}$	Sm	$\underset{122.11^{o}C}{\overset{122.23^{o}C}{\rightleftharpoons}}$	Sm'	$\underset{135.70^{o}C}{\overset{135.96^{o}C}{\rightleftharpoons}}$	I	
PEAP10	Cr	$\underset{72.47^{o}C}{\overset{93.07^{o}C}{\rightleftharpoons}}$	Sm	$\underset{145.37^{o}C}{\overset{146.15^{o}C}{\rightleftharpoons}}$	I			
PEAP12	Cr	$\underset{79.08^{o}C}{\overset{94.98^{o}C}{\rightleftharpoons}}$	Sm	$\underset{129.89^{o}C}{\overset{130.26^{o}C}{\rightleftharpoons}}$	I			
PEAP14	Cr	$\underset{75.00^{o}C}{\overset{95.54^{o}C}{\rightleftharpoons}}$	Sm	$\underset{127.09^{o}C}{\overset{127.58^{o}C}{\rightleftharpoons}}$	I			
PEAP16	Cr	$\underset{86.57^{o}C}{\overset{97.94^{o}C}{\rightleftharpoons}}$	Sm	$\underset{129.48^{o}C}{\overset{130.41^{o}C}{\rightleftharpoons}}$	I			

lengthen the rigid core unit leads to the liquid-crystal phase formation in PEAPn. Representative DSC traces for PEAP14 are shown in Figure 1. In comparison with cholest-5-ol-(3β)[4-phenylpydidylazo]carbonate (CPPC) [24], each PEAPn molecule has three aromatic rings. However, PEAPn show smectic phases, whereas CPPC is not mesogenic. Different from CPPC, each PEAPn molecule has a fully extended terminal methylene group, which facilitates an ordered arrangement to induce the

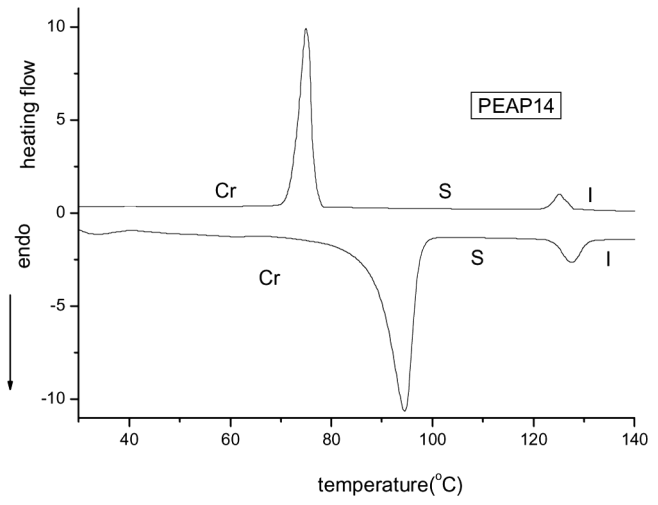

Figure 1. DSC curves of PEAP14.

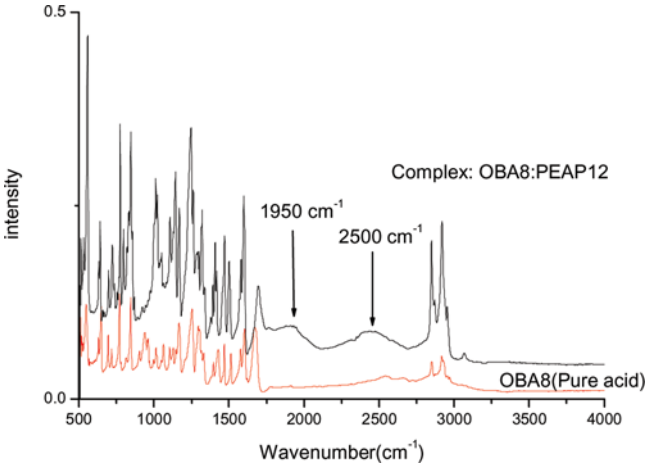

Figure 2. FTIR spectra of OBA8 and the complex OBA8:PEAP12.

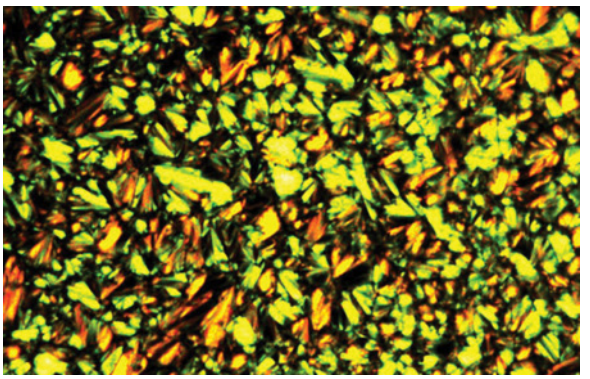

Figure 3. Microscopic texture of the complex OBA4:PEAP16 (112°C on cooling).

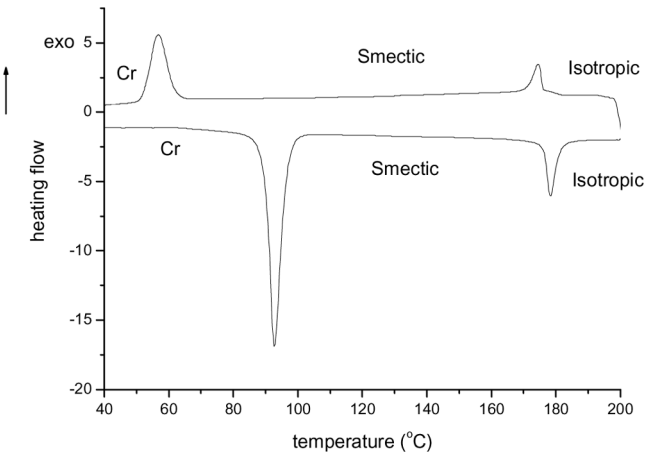

Figure 4. DSC curves of OBA7:PEAP12.

Table 4. Phase transition temperatures of OBAm: PEAPn

	OBA4:PEAPn						OBA5:PEAPn								
n=5	Cr	113.53°C / 80.13°C	Sm	195.75°C / 201.23°C	I	Cr	91.04°C / 76.99°C	Cr'	106.35°C	Sm	196.92°C / 193.00°C	I			
n=6	Cr	116.30°C / 93.62°C	Sm	197.66°C / 192.51°C	I	Cr	97.99°C / 62.80°C	Sm			190.33°C / 183.65°C	I			
n=7	Cr	115.25°C / 99.30°C	Sm	196.98°C / 192.60°C	I	Cr	95.64°C / 64.93°C	Sm			185.19°C / 184.10°C	I			
n=8	Cr	107.99°C / 69.00°C	Sm	189.68°C / 189.08°C	I	Cr	91.95°C / 65.27°C	Cr	110.21°C / 80.38°C	Sm	188.48°C / 182.64°C	I			
n=10	Cr	81.59°C / 50.04°C	Sm	183.29°C / 177.84°C	I	Cr	80.62°C / 49.68°C	Sm	171.94°C / 165.60°C	Sm'	181.66°C / 175.86°C	I			
n=12	Cr	93.71°C / 59.15°C	Sm	182.58°C / 176.88°C	I	Cr	88.03°C / 51.84°C	Sm	177.53°C / 174.04°C	Sm'	180.89°C / 177.63°C	I			
n=14	Cr	80.74°C / 48.91°C	Sm	175.65°C / 171.48°C	I	Cr	85.43°C / 43.32°C	Sm			174.43°C / 170.61°C	I			
n=16	Cr	84.63°C / 67.56°C	Sm	174.05°C / 170.04°C	I	Cr	85.26°C / 66.64°C	Sm			173.77°C / 169.65°C	I			
	OBA6:PEAPn						OBA7:PEAPn								
n=5	Cr	33.32°C / 72.00°C	Cr	101.78°C	Sm	194.50°C / 189.87°C	I	Cr	57.01°C / 74.66°C	Cr	94.23°C	Sm	188.79°C / 183.60°C	I	
n=6	Cr	99.74°C / 67.94°C	Sm	193.89°C / 189.43°C	I	Cr	109.90°C / 67.56°C	Sm			188.90°C / 186.31°C	I			
n=7	Cr	98.82°C / 67.32°C	Sm	190.64°C / 185.13°C	I	Cr	108.70°C / 66.59°C	Sm			185.71°C / 183.60°C	I			
n=8	Cr	108.83°C / 71.01°C	Sm	188.14°C / 182.71°C	I	Cr	94.02°C / 65.78°C	Sm			184.50°C / 179.27°C	I			
n=10	Cr	84.66°C / 54.43°C	Sm	182.85°C / 178.75°C	I	Cr	90.04°C / 56.69°C	Sm			180.51°C / 177.45°C	I			
n=12	Cr	85.20°C / 55.28°C	Sm	179.82°C / 176.20°C	I	Cr	92.68°C / 56.62°C	Sm			178.51°C / 174.48°C	I			
n=14	Cr	81.18°C / 41.11°C	Sm	175.25°C / 171.06°C	I	Cr	89.42°C / 43.75°C	Sm			174.83°C / 170.75°C	I			
n=16	Cr	85.45°C / 75.77°C	Sm	172.12°C / 162.35°C	I	Cr	89.04°C / 68.74°C	Sm			174.08°C / 163.77°C	I			
	OBA8:PEAPn						OBA10:PEAPn								
n=5	Cr	36.84°C / 72.67°C	Cr	94.66°C	Sm	188.31°C / 182.88°C	I	Cr	83.11°C / 78.06°C	Cr	97.47°C	Sm	182.59°C / 176.13°C	I	
n=6	Cr	109.94°C / 67.17°C	Sm	187.53°C / 182.61°C	I	Cr	91.84°C / 67.74°C	Sm			181.09°C / 175.54°C	I			
n=7	Cr	109.11°C / 65.84°C	Sm	189.40°C / 184.35°C	I	Cr	91.34°C / 74.05°C	Sm			182.47°C / 177.21°C	I			
n=8	Cr	94.25°C / 65.82°C	Sm	184.41°C / 178.69°C	I	Cr	92.85°C / 72.70°C	Sm			181.38°C / 177.92°C	I			
n=10	Cr	90.34°C / 57.14°C	Sm	180.45°C / 176.02°C	I	Cr	96.44°C / 81.67°C	Sm			177.23°C / 171.87°C	I			
n=12	Cr	92.67°C / 53.54°C	Sm	177.94°C / 173.78°C	I	Cr	94.18°C / 73.84°C	Sm			175.56°C / 171.27°C	I			
n=14	Cr	89.64°C / 43.78°C	Sm	174.81°C / 170.93°C	I	Cr	95.30°C / 42.70°C	Sm			171.40°C / 168.93°C	I			
n=16	Cr	89.46°C / 56.14°C	Sm	174.46°C / 170.46°C	I	Cr	95.36°C / 71.21°C	Sm			171.60°C / 167.28°C	I			

liquid-crystal phase. Therefore, it proves that the linearity of molecules has a profound influence on the liquid-crystal phase formation.

Mesomorphic Properties of the Complexes

The formation of the hydrogen-bonded liquid crystals, as shown in Scheme 1, was proved by Fourier transform infrared (FTIR) spectroscopy (Figure 2). The occurrence of the typical bands around 2500 and 1920 cm^{-1} [25], characteristic of the pyridine-acid complex, clearly confirmed the formation of the strong hydrogen bonding between the hydrogen acceptors and donors. Previously, the existence of the hydrogen bonding was evidently supported by single-crystal X-ray diffraction [8].

The hydrogen-bonded liquid crystals were studied by DSC and POM. All complexes examined were entiotropic smectic liquid crystals, characterized by the typical focal-conic texture. Figure 3 shows the microscopic texture of OBA4:PEAP16 investigated by POM at 112°C. Some of the complexes show two smectic phases. It is interesting to note that the thermal properties of these complexes are apparently different from those of the individual components. All the complexes exhibit a broader phase transition temperature range with a lower melting point and a much higher clear point, which clearly indicates that the hydrogen bonding can significantly stabilize the smectic phase. For example, the smectic phase range of PEAP14 is 33.04°C (from 94.54°C to 127.58°C), whereas all the series of OBAm:PEAP14 possess a smectic phase range of 76°C–94.91°C. The DSC themogram of OBA7:PEAP12 is illustrated in Figure 4.

Table 4 summarizes the phase transition temperatures of all of the hydrogen-bonded complexes. The results reveal that most of the complexes exhibit a slight odd–even effect in their mesogenic behaviors while changing the terminal chain length in either OBAm or PEAPn.

Based on the DSC results, it is evident that increasing the length of the carbon chain in OBAm and PEAPn leads to a decrease of the clear points of the complexes. Figures 5a and 5b show the dependence of the transition temperatures on the terminal chain lengths for the series of OBA10:PEAPn and OBAm:PEAP7, respectively.

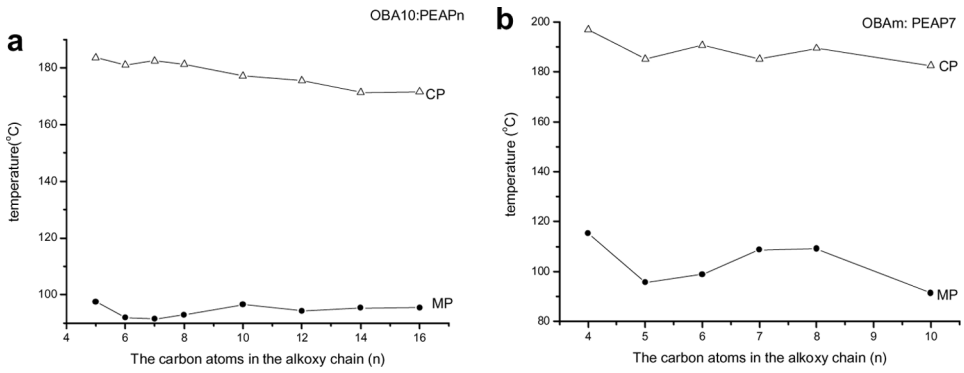

Figure 5. Plot of transition temperatures against the carbon atoms, *n*, in the alkoxyl chain for (a) series of OBA10:PEAPn, and (b) series of OBAm:PEAP7. Clear point (CP), melting point (MP).

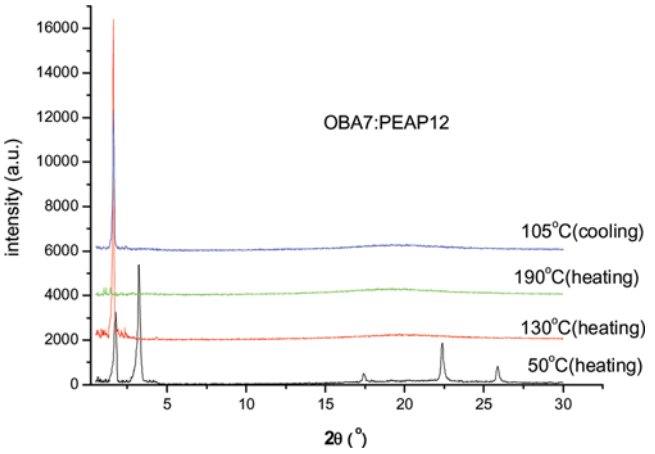

Figure 6. X-ray diffractograms of the complex OBA7:PEAP12 at different temperatures: 50°C (heating) solid; 130°C (heating) smectic; 190°C (heating) isotropic; 105°C (cooling) smectic.

Variable temperature X-ray diffraction (XRD) has proven to be an idea tool to determine the type of liquid-crystal phase. In the present study, OBA7:PEAP12 was chosen for study by powder XRD at different temperatures. Figure 6 illustrates the X-ray diffractograms of OBA7:PEAP12 observed at 50°C, 130°C, and 190°C on heating and 110°C on cooling. At 50°C, the XRD spectrum exhibits several sharp reflections at low and wide angles, implying that the complex is in a well-ordered phase as a solid. At 130°C on heating and 110°C on cooling, the existence of a broad halo at the wide angle and a sharp first-order reflection at the small angle indicates that the complex is in a smectic phase. Based on the Bragg equation $2dsin\theta = n\lambda$ (where d is the interplane distance, θ is the scattering angle, n is the order of the diffraction, and λ is the wavelength of the X-ray), the distance for the small-angle reflection was calculated to be 5.51 nm, which corresponds to the molecular length of the complex OBA7:PEAP12, and the wide angle reflection is assigned as the intermolecular distance, 0.38 nm. The calculated length of the complex OBA7:PEAP12 is 5.29 nm, which is shorter than the smectic layer spacing d. Therefore, complex OBA7:PEAP12 exhibits a typical smectic phase. At 190°C, the absence of the small-angle reflection clearly indicates that the mixture is in an isotropic phase as a liquid.

Conclusions

4′-Pyridylazophenyl-4-alkoxybenzoate compounds have been synthesized and well characterized. Supramolecuar assemblies were constructed from *para*-alkoxybenzoic acids and 4′-pyridylazophenyl-4-alkoxybenzoate and their liquid-crystal properties have been characterized by FTIR, DSC, POM, and variable-temperature XRD. All of the 4′-pyridylazophenyl-4-alkoxybenzoate compounds themselves exhibit smectic phases and the assemblies show a much wider smectic phase than their corresponding individuals. Odd–even effects were observed in most of the assemblies. The present study will provide insight into the structure–property relationship of the hydrogen-bonded liquid crystals, aiding effective constructions of azo liquid crystals for LCD applications.

References

[1] Lehn, J. M. (1988). *Angew. Chem. Int. Ed.*, *27*, 89.
[2] Bradfield, A. E., & Jones, B. (1929). *J. Chem. Soc.*, 2660.
[3] Gray, G. W., & Jones, B. (1953). *J. Chem. Soc.*, 4179.
[4] Kato, T., & Frechet, J. M. J. (1989). *J. Am. Chem. Soc.*, *111*, 8533.
[5] Paleos, C. M., & Tsiourvas, D. (2001). *Liq. Cryst.*, *28*, 1127.
[6] Gundogan, B., & Binnemans, K. (2000). *Liq. Cryst.*, *27*, 851.
[7] Lin, H. C., *et al*. (1999). *Liq. Cryst.*, *26*, 613.
[8] Song, X. Z., *et al*. (2002). *Liq. Cryst.*, *29*, 1533.
[9] Song, X. Z., Li, J. X., & Zhang, S. W. (2003). *Liq. Cryst.*, *30*, 1123.
[10] Xu, X. Y., *et al*. (2009). *Liq. Cryst.*, *36*, 1365.
[11] Kato, T., *et al*. (2006). *Liq. Cryst.*, *33*, 1434.
[12] Kato, T., & Frechet, J. M. J. (2006). *Liq. Cryst.*, *33*, 1429.
[13] Sakajiri, K., *et al*. (2009). *Chem. Lett.*, *38*, 1066.
[14] Ruslim, C., & Ichimura, K. (1998). *Chem. Lett.*, 789.
[15] Kozlovsky, M. V., *et al*. (1998). *Liq. Cryst.*, *24*, 759.
[16] Hermann, D. S., *et al*. (1997). *Phys. Rev. E*, *55*, 2857.
[17] Sasaki, T., Ikeda, T., & Ichimura, K. (1994). *J. Am. Chem. Soc.*, *116*, 625.
[18] Bauman, D., & Moryson, H. (1997). *J. Mol. Struct.*, *404*, 113.
[19] Matsui, M., *et al*. (1999). *J. Mater. Chem.*, *9*, 2755.
[20] Song, X. Z., Li, J. X., & Zhang, S. W. (2003). *Liq. Cryst.*, *30*, 331.
[21] Mallia, V. M., Antharjanam, P. K. S., & Das, S. (2003). *Liq. Cryst.*, *30*, 135.
[22] Naoum, M. M., Fahmi, A. A., & Alaasar, M. A. (2008). *Mol. Cryst. Liq. Cryst.*, *487*, 74.
[23] Naoum, M. M., Fahmi, A. A., & Alaasar, M. A. (2008). *Mol. Cryst. Liq. Cryst.*, *482*, 57.
[24] Mallia, V. A., & Das, S. (2001). *Liq. Cryst.*, *28*, 259.
[25] Kato, T., *et al*. (1993). *Liq. Cryst.*, *14*, 1311.